Computational and Theoretical Chemistry 1119 (2017) 51–58

Contents lists available at ScienceDirect

Computational and Theoretical Chemistry

journal homepage: www.elsevier.com/locate/comptc

Study of the stability of small AuRh clusters found by a Genetic Algorithm methodology

Fernando Buendía [a], Jorge A. Vargas [a], Roy L. Johnston [b], Marcela R. Beltrán [a,*]

[a] Instituto de Investigaciones en Materiales, Universidad Nacional Autónoma de México, Ciudad Universitaria, Apartado Postal 30-360, C.P. 04510 Coyoacán Ciudad de México, Mexico
[b] School of Chemistry, University of Birmingham, Edgbaston, Birmingham B15 2TT, United Kingdom

ARTICLE INFO

Article history:
Received 11 July 2017
Received in revised form 8 September 2017
Accepted 9 September 2017
Available online 11 September 2017

ABSTRACT

A comparative theoretical study has been performed on Au_mRh_n ($6 \leqslant m + n \leqslant 10$) clusters in the gas phase. The combined use of Density Functional Theory (DFT) calculations and the Mexican Enhanced Genetic Algorithm (MEGA) has been employed to efficiently explore the potential energy surface. Our results show interesting structural changes, such as the 2D-3D transformation on varying the Au:Rh composition. New structures of high stability are obtained when compared with either gold or rhodium pure clusters. The results show that the cluster properties exhibit different kind of dependencies on both the Au:Rh ratio and the cluster size.

1. Introduction

Pure gold clusters have been intensively studied in recent years due to their novel properties at the nanoscale [1–7]. It is known that relativistic effects on the electrons in gold lead to the hybridization of the 6s and 5d orbitals which generates several interesting properties such as the well documented 2-dimensionality of cluster structures up to 13 atoms [8–14]. Gold clusters have been proposed for catalysis because of their high reactivity, partly due to the high surface to volume ratio [15]. Rhodium clusters have also been studied by several groups in recent years, [16–21] and have been found to possess large magnetic moments, this phenomenon is not observed in the bulk.

The combination of two elements at the nanoscale offers the opportunity not only to tune their already useful properties by controlling their size and composition, but it also offers the opportunity to form nanoalloys. This has proved to be particularly useful to obtain better candidates for catalysis. Such is the case of the AuRh nano-alloy [22]. However, there have been only a few studies on this particular system [22–28], despite the fact that both elements have been intensively used in an independent manner in catalysis [15,29–35].

The aim of this study is to determine the structural size evolution of Au_mRh_n bimetallic clusters for the sizes $6 \leqslant m + n \leqslant 10$, such as the relation of their composition, to the observed 2D-3D transition, the behavior of the magnetic moment and the relative stability they exhibit. In Section 2 we briefly discuss the details of the DFT method and the Genetic Algorithm used in this work. Section 3 outlines the comparative study of the structural, electronic and magnetic properties for the clusters in the gas phase. Finally, we present our results and discussion in Section 4.

2. Methodology

In this work, we used the Mexican Enhanced Genetic Algorithm (MEGA) [36,37] for the search of the lowest energy isomers. This program has its roots in the BPGA, [38–40] but it was redesigned to improve its performance and functionality. Among other things, a new generator of random structures was implemented, the use of previous structures for the search was enabled, an error-proof corrector for short distances between atoms was created, more mutation types were included, but the most important was the development of efficient population rules to keep the population diversity as we detail below.

The structural minimization is performed with the VASP package, [41–44] using the generalized gradient approximation (GGA) with the Perdew-Burke-Erzenhof (PBE) exchange and correlation functional [45] and Projected Augmented Wave (PAW) pseudopotentials [46]. The energy cut-off for the plane waves has been taken at 400 eV for an adequate convergence. Methfessel-Paxton smearing, with a sigma value of 0.01 eV, was carried out to improve SCF convergence of metallic systems [47]. A spin polarizad calculation was performed to obtain the multiplicity of the clusters, VASP obtains this quantity as result of minimizing independently the α and β spin orbitals and populates them according to their ascending energy, minimizing the total energy of the system. The initial population is generated through a conjugate gradient

* Corresponding author.
E-mail address: mbeltran@servidor.unam.mx (M.R. Beltrán).

https://doi.org/10.1016/j.comptc.2017.09.008
2210-271X/

optimization (using VASP) of 10 randomly generated structures. The search is considered finished when the lowest-energy isomers of the pool remain unchanged for at least 50 steps.

Within MEGA, the application of crossover and mutation operators to a given geometry and its local relaxation is managed by independent parallel subprocesses with a global database (pool). For crossover, a pair of clusters is taken from the pool using a weighted roulette-wheel selection [40]. The offspring are then produced through single-point, weighted crossover. It is a variant of the "cut and splice" method of Deaven and Ho [48]. For mutation, two atoms of different elements are swapped generating a new homotop. In our case, 90% of the new candidates were obtained by crossover, while 10% were generated applying the "homotop" mutation operator to a structure from the pool. A key feature of MEGA is the capability of maintaining diversity in the pool [36,37]. This is achieved through a two-step procedure. First, the ordered lists of interatomic distances are compared and, in the case that all the distances differ by less than 5%, then a direct comparison of the geometries is carried out by setting the center of mass of both clusters at the origin and measuring the distances between the atoms of the different clusters while one structure is successively rotated. If a rotation is found where all the atoms of one cluster have one atom of the other cluster at a distance below a threshold value (0.4 Å), the clusters are considered similar. If the new cluster is identified to be similar to a cluster already in the pool, the program keeps only the one with the lowest energy and discards the other one. The diversity of the pool is important for two reasons: to allow a better exploration of the potential energy surface; and to obtain several different geometries (isomers). These isomers can be further minimized with another (possibly higher) level of theory which may change the energy ordering of the isomers. In order to be sure that we have enough diverse candidates, MEGA was run several times. When such methodology (using PBE) was applied on pure rhodium clusters with 4 to 12 atoms, sometimes the lowest-energy isomer in the pool does not coincide with the global minimum reported in previous combined theory-experimental studies [17,21,49,50] done with PBE0 and B3LYP respectively. This fact proves that the use of hybrid functionals (like PBE0) is necessary to obtain the correct lowest-energy isomers.

Nonetheless, we have found that the final pool contains the true minimum [21] in all cases, but as higher-energy isomer. This behavior is shown in Fig. 1 for the Rh_8 case, comparing the results obtained with PBE and the hybrid PBE0. On the other hand, for pure gold clusters such dependence of the ordering of the isomers with these functionals is not observed at the sizes studied here [51].

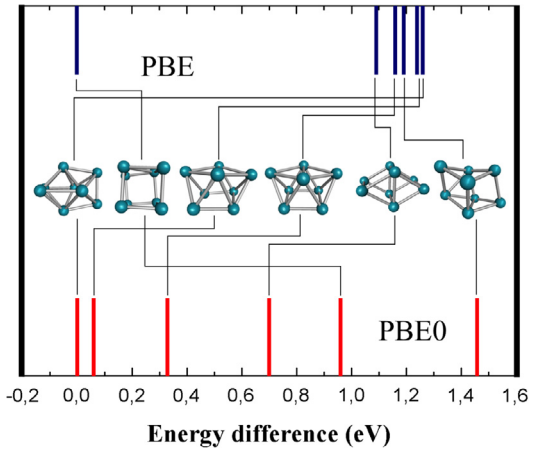

Fig. 1. Order of lowest-energy isomers for Rh_8 with the PBE and the PBE0 functional.

This result led to a subsequent minimization using the Turbomole package [52] with the hybrid PBE0 functional [53] of all the isomers present in our final pool. These calculations were performed using a def2-TZVP basis set [54] and studying the multiplicity of the isomers and four neighboring multiplicities around the ground state. Finally, to confirm that the structures are local minima, we calculated the vibrational normal modes. The charge population was calculated using the natural bond orbital approximation [55]. We have calculated certain energetic values that help to understand the stability of the clusters. The binding energy per atom is obtained as:

$$E_b/atom = E(\mathrm{Au}_m\mathrm{Rh}_n) - [mE(\mathrm{Au}) + nE(\mathrm{Rh})] \quad (1)$$

We have also used the excess energy (Δ) to determine the stability of the bimetallic clusters relative to pure gold and rhodium clusters. This quantity is defined as:

$$\Delta = E(\mathrm{Au}_m\mathrm{Rh}_n) - [(n/N)E(\mathrm{Au}_N) + (m/N)E(\mathrm{Rh}_N)] \quad (2)$$

where N = m + n. The physical meaning of this value is easy to understand, it is the energy of the mixed cluster with respect to pure clusters of the same size, a negative value of Δ implies favorable mixing [56].

3. Results

We first analyzed the case of pure gold and rhodium clusters to test how well the two functionals used in this work (PBE and PBE0) behave. These results are shown in Fig. 2. For gold, the lowest energy isomers exhibit the characteristic odd-even stability and planarity when calculated with PBE. These characteristics are maintained when PBE0 is employed. On the contrary, the lowest-energy rhodium isomers have non-planar structures, but we observed that the structures obtained first with PBE (cubic structures) differ from those obtained with PBE0 (rombohedral structures). The latter are clearly in better agreement with experimental Far InfraRed Multi-Photon Dissociation (FIR-MPD) results [21]. The magnetic moment and the binding energy per atom steadily increase with the number of atoms in this size range. With this analyses, we can conclude that geometry reoptimization with PBE0 maintains the planarity of the gold clusters and also gives the correct geometries for rhodium. This is an important point to prove the reliability of our methodology as we are going to study cluster sizes where there is insufficient experimental data for comparison. The structures of the lowest and second lowest energy isomers for the Au_mRh_n (n + m = 6–10) clusters are shown in Figs. 3–5, and the multiplicities, excess energies and binding energies are shown in Figs. 6–8.

3.1. 6 atoms

The lowest energy isomers for the systems with higher gold concentrations are triangular structures (Au_5Rh and Au_4Rh_2) due to the well-known s-d hybridization of the gold atoms, while the clusters with higher rhodium concentration generate pyramids of rhodium capped with gold atoms (Au_2Rh_4, $AuRh_5$). The case of Au_3Rh_3 is especially interesting because the lowest energy isomer is a 3D distorted triangle and, when we constrained the structure to be 2D, although the s-d hybridization was enhanced, we found the energy to be 0.21 eV higher than for the distorted structure. The two Au_2Rh_4 clusters shown in 3 have the same structure, but with different multiplicity (M = 7 and M = 9) and the energy difference between them is 0.24 eV. The other isomers for all the 6-atom systems are high in energy ($\Delta E > 0.3$ eV). The magnetic moment increases with the rhodium concentration, almost in a monotonical manner, ranging from 2 μ_B for Au_5Rh to 8 μ_B for $AuRh_5$. This

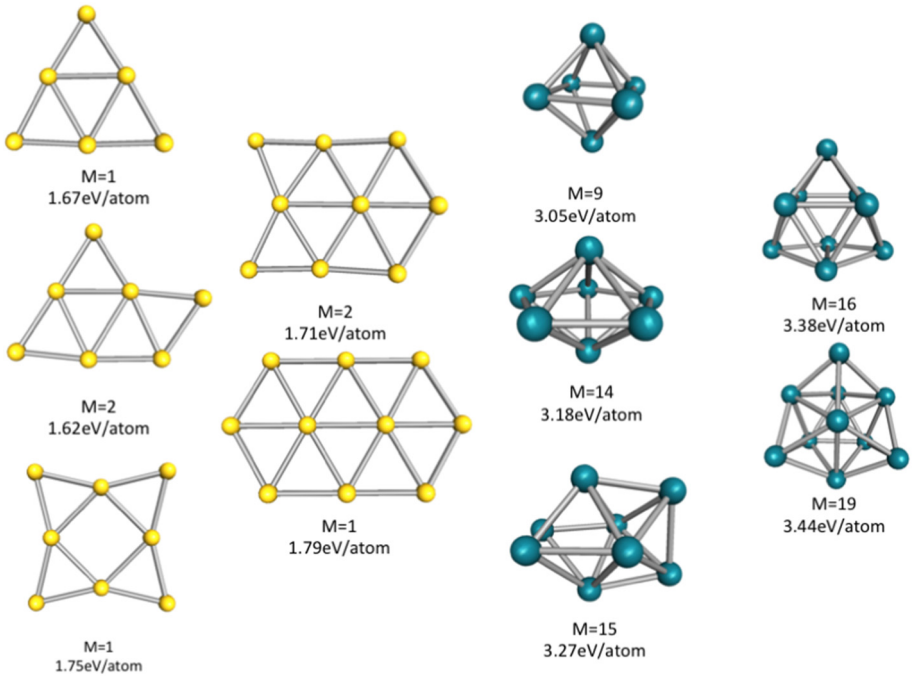

Fig. 2. Lowest energy isomers for Au_n and Rh_n (n = 6–10) with their spin multiplicities (M) and their binding energies per atom (obtained at the PBE0/def2-TZVP level).

behavior is related to some rhodium d-orbitals in the cluster which are not involved in cluster bonding and in which the electrons are not paired. For nearly all compositions, the excess energies are positive, suggesting that the mixed clusters are less favored with respect to homo-atomic clusters: only Au_3Rh_3 is more stable than the pure clusters, with an excess energy of −0.08 eV. The reason for this result is that both, Au_6 and Rh_6 represent relatively very stable clusters with quite different structures, the first is a 2D triangle, while the latter forms a 3D octahedron. A similar finding has been reported for 6-atom AuPd clusters [57].

3.2. 7 atoms

There are two hexagonal planar lowest-energy isomers for the systems with higher gold concentrations (Au_6Rh and Au_5Rh_2). The energy differences between these two systems and the 3-dimensional structures are 0.76 eV and 0.13 eV, respectively. On the other hand, Au_4Rh_3, Au_3Rh_4 and Au_2Rh_5 form bi-capped trigonal bi-pyramids with the rhodium atoms in central positions. This is due to the higher binding energy of Rh. The smallest energy difference between the 3D and 2D lowest-energy isomers for Au_4Rh_3 is 0.68 eV. Finally, the lowest energy structure for $AuRh_6$ has an Rh_6 octahedron capped by a gold atom. The 7-atom structures are formed of an inner core of rhodium atoms surrounded by gold atoms. For all systems studied here, the multiplicity monotonically increases with rhodium concentration; yet only Au_2Rh_5 and $AuRh_6$ have the same multiplicity (M = 10). The excess energy analysis shows that the 6 systems prefer to form alloys of the two different atoms rather than to form homo-nuclear clusters. This agrees with the fact that pure systems with an odd number of atoms are less stable.

3.3. 8 atoms

The systems with 8 atoms only have one planar structure (Au_7Rh) as a lowest energy isomer; its planarity is due to increased s-orbital character in the bonding. Even for this cluster, the difference between the lowest-energy 2D and 3D isomers is small (0.15 eV). The lowest energy isomers for Au_6Rh_2, Au_5Rh_3 and Au_4Rh_4 have similar 3D structures, with the rhodium atoms located at high coordinated sites. For Au_6Rh_2 the energy difference between the planar and non-planar structures is only 0.04 eV. The geometries of the systems with higher rhodium concentrations are very similar to the pure rhodium clusters but with gold atoms in the low-coordinate capping positions. The Rh core consists of a triangle for the 3 Rh system, a tetrahedron for 4 atoms, a square pyramid for 5 and an octahedron for 6 Rh atoms. The second isomers are closer to the lowest energy isomers than those of the 6- and 7-atom systems; even the clusters Au_6Rh_2 and Au_5Rh_3 have isomers within 0.1 eV of the lowest energy isomer. Only four clusters with 8 atoms have negative excess energies, which is lower than the 7-atom systems, which shows their low capacity to create mixed alloys compared with the previous sizes. This behavior is due to the high stability of the planar Au_8 and 3D bi-capped octahedron Rh_8 clusters.

3.4. 9 atoms

Several 9-atom clusters have one or two isomers which lie very close in energy to the lowest energy isomer and in two cases the energy gap is less than the thermal energy at room temperature ($\Delta E < k_BT$). This is related to the large number of combinations that can be created with more atoms and its homotopic configurations. All the mixed clusters are three-dimensional, which is different from the findings for smaller clusters. In the case of Au_8Rh, a 2D structure might reasonably be expected. However, as the best 2D structure lies 0.2 eV above the lowest energy 3D structure, this could be a result of the high stability of Au_6Rh, which has the largest negative value for the excess energy of all the Au_nRh structures studied here and is the basis of the 3D Au_8Rh structure. For Au_4Rh_5 and Au_3Rh_6, the lowest energy isomers are tri-capped octahedra. Three systems (Au_7Rh_2, Au_5Rh_4 and Au_2Rh_7) have as global minima bi-capped pentagonal bi-pyramid structures. This motif is the most stable for these three systems, even though the rhodium concentration is very different in each case. All these systems are distorted due to the difference in Au-Au, Au-Rh and Rh-Rh bond lengths. For larger rhodium concentrations, there is an inner core of Rh capped by Au atoms. This is confirmed in experiments

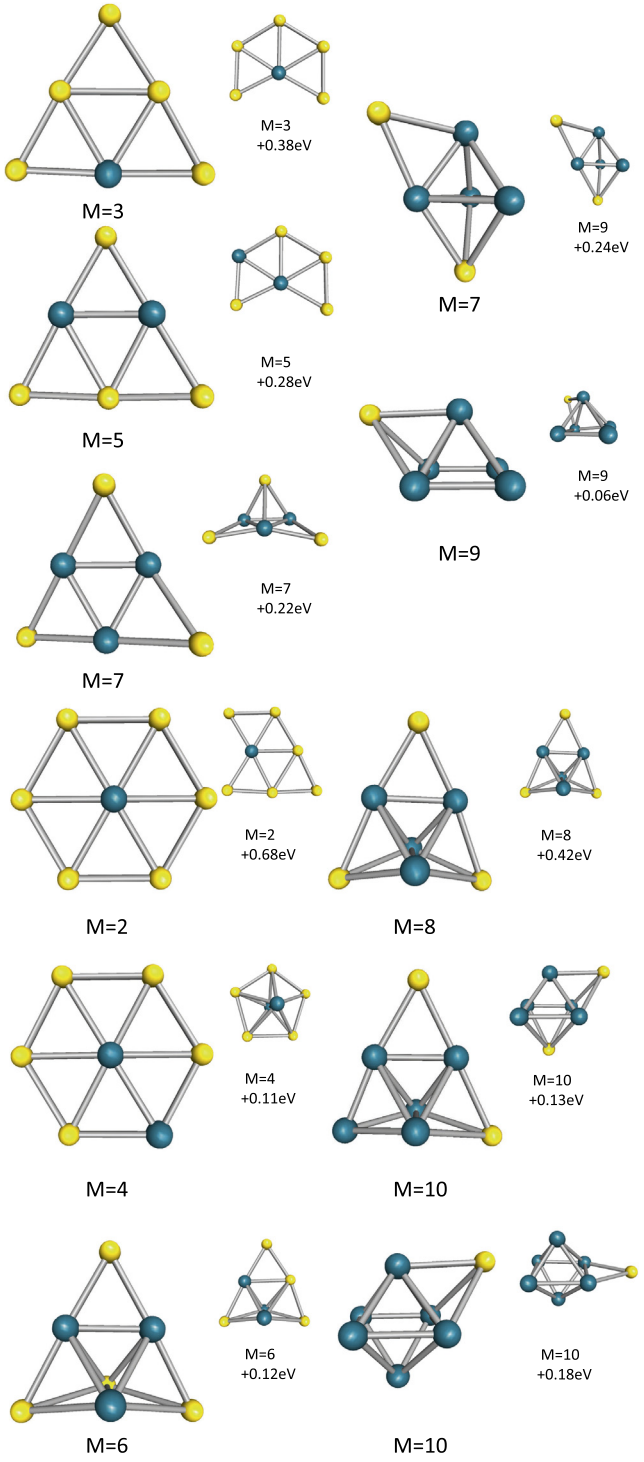

Fig. 3. First and second lowest energy isomers for Au_mRh_n (n + m = 6, 7), with their spin multiplicites (M) and the energy difference in (eV) with respect to the lowest energy isomer (obtained at the PBE0/def2-TZVP level).

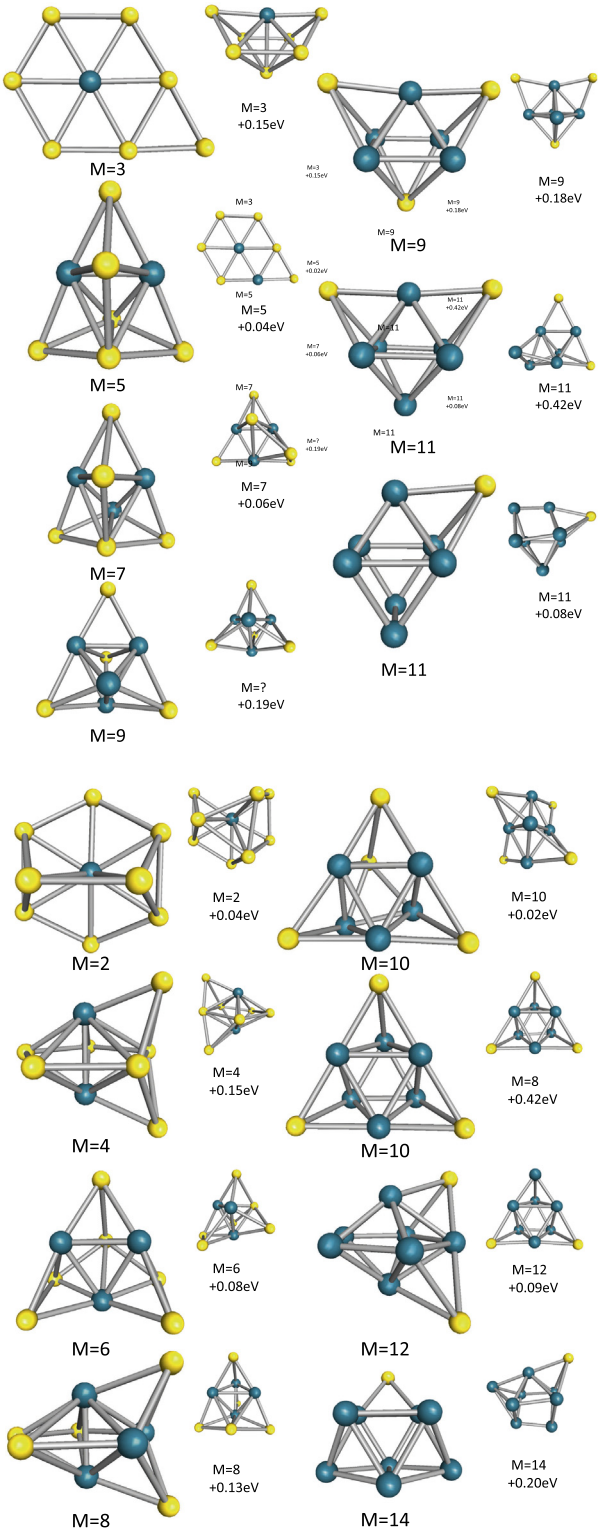

Fig. 4. First and second lowest energy isomers for Au_mRh_n (n + m = 8, 9) with their spin multiplicities and the energy difference in (eV) with respect to the lowest energy isomer (obtained at the PBE0/def2-TZVP level).

on larger sizes [58]. Eight compositions for this size show favorable mixing (negative excess energies). It seems that an increase in cluster size leads to an increase in the number of mixed clusters that have negative excess energy.

3.5. 10 atoms

For the 10-atom system, only Au_9Rh is planar. This planar cluster has a charge transfer 0.09 e from the rhodium atom towards the gold atoms, while the second energy isomer (which has a 3D structure) shows the reverse effect, with a charge transfer of 1.22e from the gold atoms towards the rhodium atom. This is due to energy lowering of the Rh 4d orbitals when the cluster is 3D, which enables Au (5s) to Rh (4d) electron transfer. We can see the same effect, only slightly smaller, for Au_8Rh_2, where there is charge

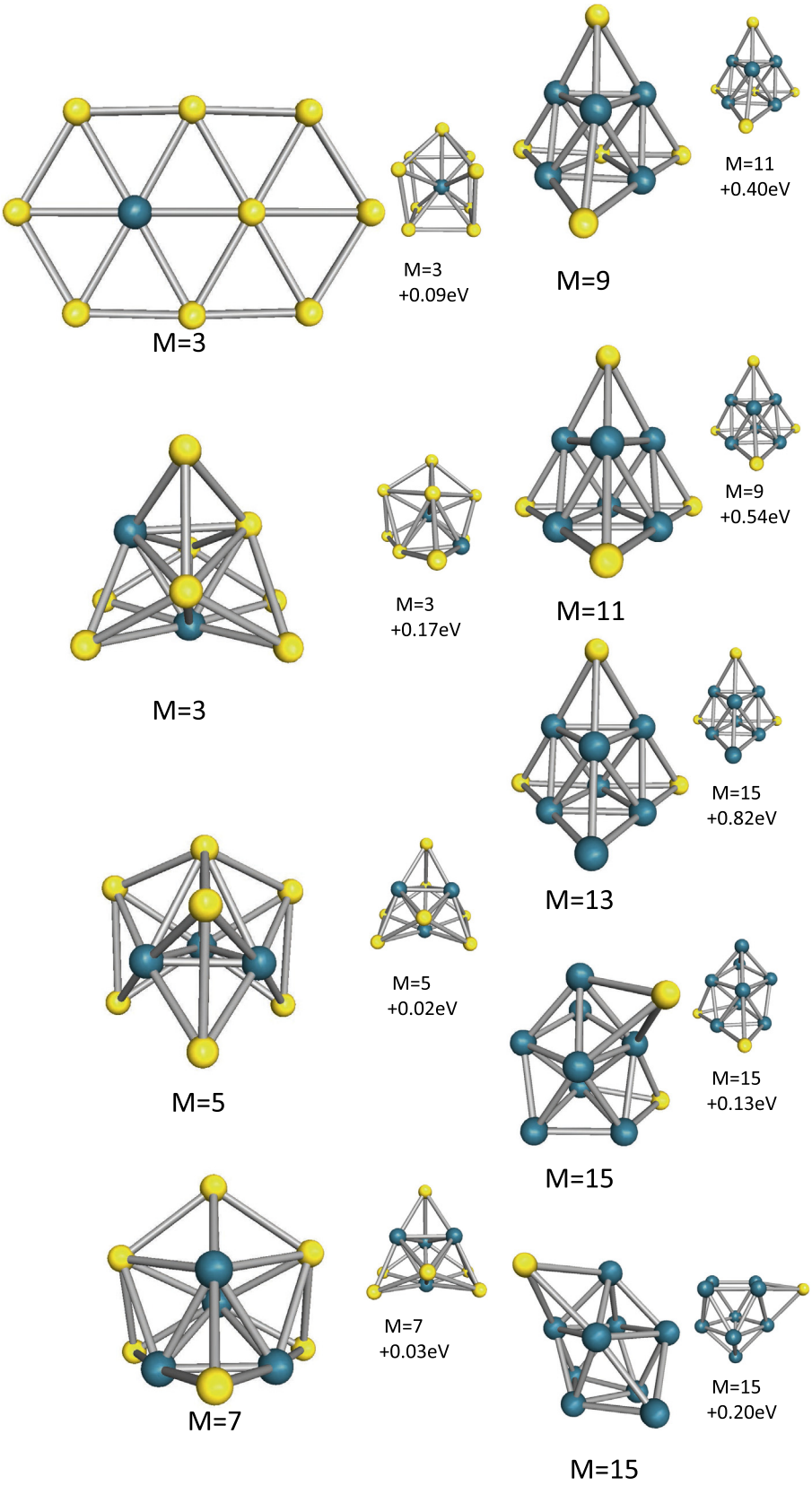

Fig. 5. First and second lowest energy isomers for Au_mRh_n (n + m = 10) with their spin multiplicities and the energy difference in (eV) with respect to the lowest energy isomer (obtained at the PBE0/def2-TZVP level).

transfer to the gold atoms of 0.12e in the lowest 2D isomer and 0.54e for the lowest 3D isomer (these results are shown in Table 1). For Au_6Rh_4 the lowest-energy isomer is similar to a tetrahedron, although, one triangular face of 6 atoms is modified to maximize the number of bonds with the rhodium atom. On the other hand, the next clusters with higher rhodium concentration (Au_5Rh_5,

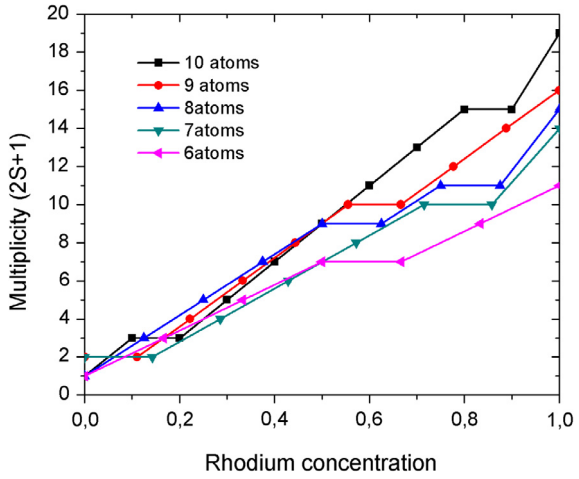

Fig. 6. Spin multiplicities for the lowest energy isomers of $Au_{N-n}Rh_n$ (N = 6–10, n = 0-N).

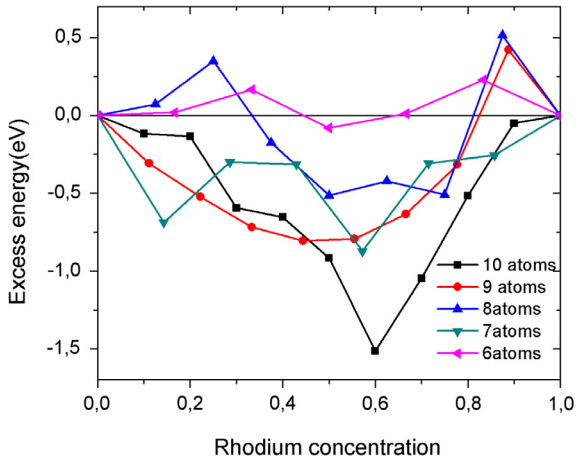

Fig. 7. Excess energies for the lowest energy isomers of $Au_{N-n}Rh_n$ (N = 6–10, n = 0-N).

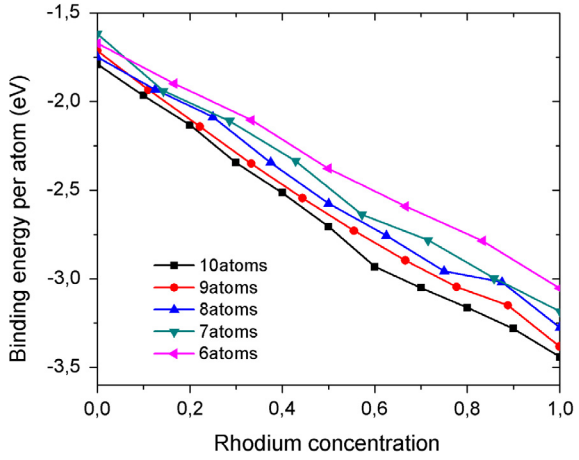

Fig. 8. Binding energies per atom for the lowest energy isomers of $Au_{N-n}Rh_n$ (N = 6–10, n = 0-N).

Au_4Rh_6 and Au_3Rh_7) show a slightly distorted tetrahedral motif for the lowest energy isomer, with an inner core of rhodium atoms. For these clusters, the charge is transferred from the inner rhodium cluster to the gold atoms, due to the higher electronegativity of the isolated low-coordinate gold atoms. Finally, Au_2Rh_8 and $AuRh_9$ do not form the tetrahedral structure. For these 10-atom systems, the second isomers are again close in energy to the lowest energy isomers. The increase in the multiplicity is quasi-linear with the increase of the rhodium concentration. There are two mixed clusters with the maximum multiplicity for the clusters studied here (Au_2Rh_8 and $AuRh_9$, with 14 unpaired electrons and M = 15). This is the only size where the mixing process is favorable (negative excess energy) for all compositions.

Table 1
Comparison of (electron) charge transfer from the gold atoms to the rhodium atom(s) for several gold-rich clusters; a negative value means the charge transfer is from the rhodium atom(s) towards the gold atoms.

Cluster	Charge transfer	
	2D	3D
Au_6Rh_2	−0.14	−0.41
Au_7Rh	0.06	−0.03
Au_7Rh_2	0.14	−0.16
Au_8Rh	0.49	0.14
Au_8Rh_2	0.54	0.12
Au_9Rh	1.22	−0.09

4. Conclusions

The increase in cluster size favors three-dimensional structures as the lowest-energy isomers; even for systems with 9 atoms no planar structures are found as the lowest-energy isomers. The study of electronic charges explains why these transformations occur; clusters such as Au_3Rh_3 are representative of the relation between the decrease of the d-character of the bonding and the 2D to 3D transformation. The 8, 9 and 10-atom systems with low rhodium concentrations show how the 3D structures exhibit electron transfer from the gold to the rhodium atoms due to a slight charge transfer from the Au 5s orbital to Rh 4d orbitals (as can be seen in Table 1). The systems with high concentrations of gold favor planar clusters similar to Au_n, with the rhodium atoms located in high coordinated sites. These structures are distorted due to the difference in size of the atoms (this effect is shown for several systems in Fig. 9). Regarding the charge, we observed electron transfer from the rhodium atoms to the gold atoms for the planar clusters and vice versa for the non-planar structures, with the magnitude of electron transfer increases with cluster size. On the other hand, the clusters with high concentrations of rhodium form structures made of an inner rhodium core (similar to the Rh_n lowest energy isomers) with the gold atoms forming an outer (albeit partial) shell; this effect is shown for several systems in Fig. 10.

The presence of the rhodium atoms drastically reduces the stability of the planar clusters. In these cases, we observe a transfer of charge from the inner rhodium core towards the peripheral gold atoms due to the higher electronegativity of the gold atoms. The tendency to form mixed clusters increases with cluster size for clusters with even numbers of atoms. For clusters with 6, 8 and 10 atoms there are 4 and 3 and 0 lowest energy isomers, respectively, that do not exhibit favorable mixing. All the clusters with 10 atoms show large negative values for the excess energy, this is due to the high stability of the distorted and non-distorted tetrahedral motifs. Here we would like to highlight that this type of structure is new for mixed systems of this size, and represents and important property for bimetallic clusters.

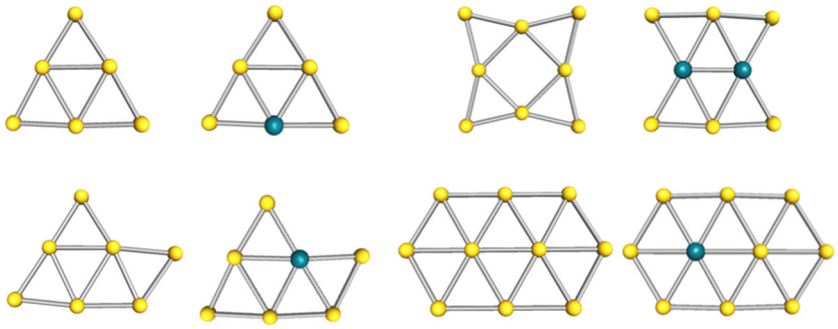

Fig. 9. Au_n clusters and singly-Rh-doped analogues that have the same structures, with the rhodium atoms in high-coordinated sites.

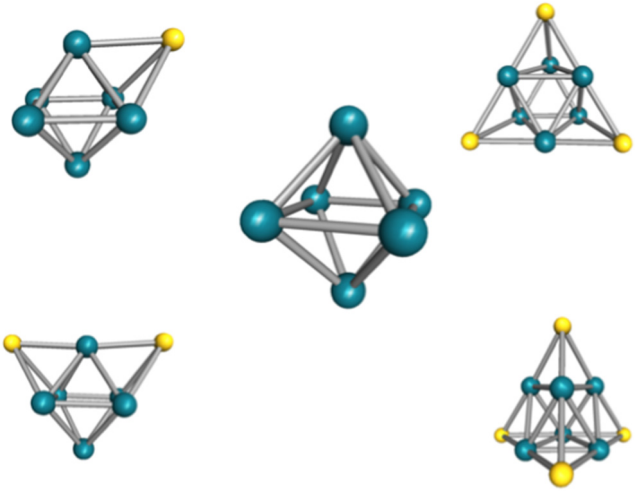

Fig. 10. Lowest energy isomers for Rh_6, $AuRh_6$, Au_2Rh_6, Au_3Rh_6 and Au_3Rh_6, where the same inner octahedral (Rh_6) motif is maintained.

All odd numbered clusters show negative excess energies. The relatively higher capacity to create mixed clusters can be explained by the fact that Au_{2n+1} and Rh_{2n+1} clusters are less stable. As both Au and Rh are odd-electron atoms, these odd-atom clusters also have odd numbers of electrons, so they cannot be closed shell magic number clusters. For all the sizes studied here, we observe that the most favorable mixing occurs when the concentration ratio Au:Rh is around 50%. The number of low-lying isomers is generally larger at this composition, largely because the number of homotops is maximised for these compositions. Both the binding energy and the number of unpaired electrons increase with the rhodium concentration. The increase of the binding energy confirms the expected behavior of E_b(Rh-Rh) > E_b(Au-Rh) > E_b(Au-Au). On the other hand, the increase of the magnetic moment is related to the rhodium d-orbitals that do not contribute to the cluster bonding. The use of MEGA has proven to be useful, firstly because we can study many points of the energy surface that may be missed when the search is done in an empirical manner. The second reason is that the new implementation maintains the diversity in the pool. When these structures are re-optimized with the PBE0 hybrid functional and larger basis set, we observe changes in the order of the isomers. Nevertheless the Genetic Algorithm code has been applied several times to form a sufficiently diverse pool to be confident that it contains the true global minima at least in the size range here studied. This has been corroborated at least for the pure gold and pure rhodium clusters when compared with experimental results [8–12,17,21].

Acknowledgments

We acknowledge support from PAPIIT IN100515, UNAM project. F.B. acknowledges support from CONACYT (financial support No. 379750). J.A.V. acknowledges a postdoctoral grant from DGAPA UNAM. We thank Alberto López Vivas for his technical support, and R.L.J. acknowledge the Engineering and Physical Sciences Research Council, U.K. (EPSRC), for funding under Critical Mass Grant EP/J010804/1 TOUCAN: Towards an Understanding of Catalysis on Nanoalloys. Calculations were performed via membership of the U.K.'s HPC Materials Chemistry Consortium, which is funded by EPSRC (EP/L000202); this work made use of the facilities of ARCHER, the U.K.'s national high performance computing service, which is funded by the Office of Science and Technology through EPSRC's High End Computing Programme.

Appendix A. Supplementary material

Supplementary data associated with this article can be found, in the online version, at http://dx.doi.org/10.1016/j.comptc.2017.09.008.

References

[1] I.L. Garzón, K. Michaelian, M.R. Beltrán, A. Posada-Amarillas, P. Ordejón, E. Artacho, D. Sánchez-Portal, J.M. Soler, Lowest energy structures of gold nanoclusters, Phys. Rev. Lett. 81 (1998) 1600–1603.
[2] J.M. Soler, M.R. Beltrán, K. Michaelian, I.L. Garzón, P. Ordejón, D. Sánchez-Portal, E. Artacho, Metallic bonding and cluster structure, Phys. Rev. B 61 (2000) 5771–5780.
[3] I.L. Garzón, J.A. Reyes-Nava, J.I. Rodríguez-Hernández, I. Sigal, M.R. Beltrán, K. Michaelian, Chirality in bare and passivated gold nanoclusters, Phys. Rev. B 66 (2002) 073403.
[4] M.R. Beltrán, R. Suárez Raspopov, G. González, Structural evolution study of 1-2 nm gold clusters, Eur. Phys. J. D 65 (2011) 411–420.
[5] I.L. Garzón, M.R. Beltrán, G. González, I. Gutíerrez-González, K. Michaelian, J.A. Reyes-Nava, J.I. Rodríguez-Hernández, Chirality, defects, and disorder in gold clusters, Eur. Phys. J. D 24 (2003) 105–109.
[6] R.L. Chantry, S.L. Horswell, Z.Y. Li, R.L. Johnston, Interfacial structures and bonding in metal-coated gold nanorods, Struct. Bond. 162 (2014) 67–90.
[7] H. Häkkinen, U. Landman, Gold clusters (au_N, 2-10) and their anions, Phys. Rev. B 62 (2000) R2287–R2290.
[8] P. Gruene, B. Butschke, J. Lyon, D.M. Rayner, A. Fielicke, Far-ir spectra of small neutral gold clusters in the gas phase, Z. Phys. Chem. 228 (2014) 337–350.
[9] P. Gruene, D.M. Rayner, B. Redlich, A.F.G. Van der Meer, J.T. Lyon, G. Meijer, A. Fielicke, Structures of neutral Au7, Au19, and Au20 clusters in the gas phase, Science 321 (2008) 674–676.
[10] L.M. Ghiringhelli, P. Gruene, J.T. Lyon, D.M. Rayner, G. Meijer, A. Fielicke, M. Scheffler, Not so loosely bound rare gas atoms: finite-temperature vibrational fingerprints of neutral gold-cluster complexes, New J. Phys. 15 (2013) 083003.
[11] C. Jackschath, I. Rabin, W. Schulze, Electronic structures and related properties. Electron impact ionization potentials of gold and silver clusters Me_n, $n \leq 22$, Berichte der Bunsengesellschaft fr physikalische Chemie 96 (1992) 1200–1204.
[12] D. Schooss, P. Weis, O. Hampe, M.M. Kappes, Determining the size-dependent structure of ligand-free gold-cluster ions, Philos. Trans. Roy. Soc. London A: Math. Phys. Eng. Sci. 368 (2010) 1211–1243.

[13] L.-M. Wang, L.-S. Wang, Probing the electronic properties and structural evolution of anionic gold clusters in the gas phase, Nanoscale 4 (2012) 4038–4053.
[14] G. Bravo-Pérez, I. Garzón, O. Novaro, Ab initio study of small gold clusters, J. Mol. Struct.: {THEOCHEM} 493 (1999) 225–231.
[15] M. Haruta, Size- and support-dependency in the catalysis of gold, Catal. Today 36 (1997) 153–166.
[16] F. Aguilera-Granja, J.L. Rodríguez-López, K. Michaelian, E.O. Berlanga-Ramírez, A. Vega, Structure and magnetism of small rhodium clusters, Phys. Rev. B 66 (2002) 224410.
[17] M.R. Beltrán, F. Buendía Zamudio, V. Chauhan, P. Sen, H. Wang, Y.J. Ko, K. Bowen, Ab initio and anion photoelectron studies of Rh_n (n = 1 – 9) clusters, Eur. Phys. J. D 67 (2013) 1–8.
[18] B.V. Reddy, S.N. Khanna, B.I. Dunlap, Giant magnetic moments in 4 *d* clusters, Phys. Rev. Lett. 70 (1993) 3323–3326.
[19] B.V. Reddy, S.K. Nayak, S.N. Khanna, B.K. Rao, P. Jena, Electronic structure and magnetism of Rh_n (n=2-13) clusters, Phys. Rev. B 59 (1999) 5214–5222.
[20] Y.-C. Bae, H. Osanai, V. Kumar, Y. Kawazoe, Nonicosahedral growth and magnetic behavior of rhodium clusters, Phys. Rev. B 70 (2004) 195413.
[21] D.J. Harding, P. Gruene, M. Haertelt, G. Meijer, A. Fielické, S.M. Hamilton, W.S. Hopkins, S.R. Mackenzie, S.P. Neville, T.R. Walsh, Probing the structures of gas-phase rhodium cluster cations by far-infrared spectroscopy, J. Chem. Phys. 133 (2010) 214304.
[22] F. Buendía, R.M. Beltrán, O2 adsorption on Au_nRh n = 1–5 neutral and charged clusters, Eur. Phys. J. D 70 (2016) 1–9.
[23] J.-X. Yang, C.F. Wei, J.J. Guo, Density functional study of AunRh (n = 1–8) clusters, Physica B: Phys. Condensed Matter 405 (2010) 4892–4896.
[24] F. Buendía, M.R. Beltrán, X. Zhang, G. Liu, A. Buytendyk, K. Bowen, Ab initio and anion photoelectron study of Au_nRh_m (n = 1–7, m = 1–2) clusters, Phys. Chem. Chem. Phys. 17 (2015) 28219–28227.
[25] I. Demiroglu, Z.Y. Li, L. Piccolo, R.L. Johnston, A DFT study of molecular adsorption on Au-Rh nanoalloys, Catal. Sci. Technol. 6 (2016) 6916–6931.
[26] L. Piccolo, Z.Y. Li, I. Demiroglu, F. Moyon, Z. Konuspayeva, G. Berhault, P. Afanasiev, W. Lefebvre, J. Yuan, R.L. Johnston, Understanding and controlling the structure and segregation behaviour of AuRh nanocatalysts, Sci. Rep. 6 (2016) 35226.
[27] I. Demiroglu, Z.Y. Li, L. Piccolo, R.L. Johnston, A DFT study of molecular adsorption on titania-supported AuRh nanoalloys, Comput. Theor. Chem. (2017) 142–151.
[28] F. Buendía, J.A. Vargas, M.R. Beltran, J.B.A. Davis, R.L. Johnston, A comparative study of Au_mRh_n ($4 \leq m + n \leq 6$) clusters in the gas phase versus those deposited on (100) mgo, Phys. Chem. Chem. Phys. 18 (2016) 22122–22128.
[29] W.T. Wallace, R.B. Wyrwas, R.L. Whetten, R. Mitrić, V. Bonačić-Koutecký, Oxygen adsorption on hydrated gold cluster anions: Experiment and theory, J. Am. Chem. Soc. 125 (2003) 8408–8414.
[30] W.T. Wallace, R.B. Wyrwas, R.L. Whetten, R. Mitrić, V. Bonačić-Koutecký, Oxygen adsorption on hydrated gold cluster anions: experiment and theory, J. Am. Chem. Soc. 125 (2003) 8408–8414.
[31] W.T. Wallace, R.L. Whetten, Coadsorption of CO and O_2 on selected gold clusters: evidence for efficient room-temperature CO_2 generation, J. Am. Chem. Soc. 124 (2002) 7499–7505.
[32] C. Bürgel, N.M. Reilly, G.E. Johnson, R. Mitrić, M.L. Kimble, J.A.W. Castleman, V. Bonačić-Koutecký, Influence of charge state on the mechanism of co oxidation on gold clusters, J. Am. Chem. Soc. 130 (2008) 1694–1698.
[33] G.E. Johnson, R. Mitrić, V. Bonačić-Koutecký, J.A.W. Castleman, Clusters as model systems for investigating nanoscale oxidation catalysis, Chem. Phys. Lett. 475 (2009) 1–9.
[34] F. Wang, D. Zhang, X. Xu, Y. Ding, Theoretical study of the co oxidation mediated by Au_3^+, Au_3, and Au_3^-: Mechanism and charge state effect of gold on its catalytic activity, J. Phys. Chem. C 113 (2009) 18032–18039.
[35] H. Francisco, V. Bertin, J.R. Soto, M. Castro, Charge and geometrical effects on the catalytic n2o reduction by rh6- and rh6+ clusters, J. Phys. Chem. C 120 (2016) 23648–23659.
[36] J.A. Vargas, F. Buendía, R.M. Beltrán, New Au_N (N = 27-30) lowest energy clusters obtained by means of an improved dft-genetic algorithm methodology, J. Phys. Chem. C 121 (2017) 10982–10991.
[37] J.A. Vargas, F. Buendía, R.M. Beltrán, Optimizing the search for global minima of atomic clusters through a DFT-Genetic Algorithm, (2017).
[38] https://bitbucket.org/jbadavis/bpga/.
[39] A. Shayeghi, D. Gotz, J.B.A. Davis, R. Schafer, R.L. Johnston, Pool-BCGA: a parallelised generation-free genetic algorithm for the ab initio global optimisation of nanoalloy clusters, Phys. Chem. Chem. Phys. 17 (2015) 2104–2112.
[40] R.L. Johnston, Evolving better nanoparticles: genetic algorithms for optimising cluster geometries, Dalton Trans. (2003) 4193–4207.
[41] G. Kresse, J. Hafner, *Ab initio* molecular dynamics for liquid metals, Phys. Rev. B 47 (1993) 558–561.
[42] G. Kresse, J. Hafner, *Ab initio* molecular-dynamics simulation of the liquid-metal amorphous-semiconductor transition in germanium, Phys. Rev. B 49 (1994) 14251–14269.
[43] G. Kresse, J. Furthmüller, Efficiency of ab-initio total energy calculations for metals and semiconductors using a plane-wave basis set, Comput. Mater. Sci. 6 (1996) 15–50.
[44] G. Kresse, J. Furthmüller, Efficient iterative schemes for *ab initio* total-energy calculations using a plane-wave basis set, Phys. Rev. B 54 (1996) 11169–11186.
[45] J.P. Perdew, K. Burke, Y. Wang, Generalized gradient approximation for the exchange-correlation hole of a many-electron system, Phys. Rev. B 54 (1996) 16533–16539.
[46] G. Kresse, D. Joubert, From ultrasoft pseudopotentials to the projector augmented-wave method, Phys. Rev. B 59 (1999) 1758–1775.
[47] M. Methfessel, A.T. Paxton, High-precision sampling for Brillouin-zone integration in metals, Phys. Rev. B 40 (1989) 3616–3621.
[48] D.M. Deaven, K.M. Ho, Molecular geometry optimization with a genetic algorithm, Phys. Rev. Lett. 75 (1995) 288–291.
[49] D.J. Harding, T.R. Walsh, S.M. Hamilton, W.S. Hopkins, S.R. Mackenzie, P. Gruene, M. Haertelt, G. Meijer, A. Fielicke, Communications: the structure of rh8+ in the gas phase, J. Chem. Phys. 132 (2010) 011101.
[50] J.L.F. Da Silva, M.J. Piotrowski, F. Aguilera-Granja, Hybrid density functional study of small rh_n ($n = 2 - 15$) clusters, Phys. Rev. B 86 (2012) 125430.
[51] S. Gilb, P. Weis, F. Furche, R. Ahlrichs, M.M. Kappes, Structures of small gold cluster cations (aun+, n<14): Ion mobility measurements versus density functional calculations, J. Chem. Phys. 116 (2002) 4094–4101.
[52] R. Ahlrichs, M. Bär, M. Haser, H. Horn, C. Kölmel, Electronic structure calculations on workstation computers: the program system turbomole, Chem. Phys. Lett. 162 (1989) 165–169.
[53] J.P. Perdew, M. Ernzerhof, K. Burke, Rationale for mixing exact exchange with density functional approximations, J. Chem. Phys. 105 (1996) 9982–9985.
[54] F. Weigend, R. Ahlrichs, Balanced basis sets of split valence, triple zeta valence and quadruple zeta valence quality for H to Rn: Design and assessment of accuracy, Phys. Chem. Chem. Phys. 7 (2005) 3297–3305.
[55] P.-O. Löwdin, Quantum theory of many-particle systems. ii. study of the ordinary hartree-fock approximation, Phys. Rev. 97 (1955) 1490–1508.
[56] J.B.A. Davis, S.L. Horswell, R.L. Johnston, Application of a parallel genetic algorithm to the global optimization of gas-phase and supported gold-iridium sub-nanoalloys, J. Phys. Chem. C 120 (2016) 3759–3765.
[57] H.A. Hussein, J.B.A. Davis, R.L. Johnston, Dft global optimisation of gas-phase and mgo-supported sub-nanometre aupd clusters, Phys. Chem. Chem. Phys. 18 (2016) 26133–26143.
[58] L. Piccolo, Z. Li, I. Demiroglu, F. Moyon, Z. Konuspayeva, G. Berhault, P. Afanasiev, W. Lefebvre, J. Yuan, R.L. Johnston, Understanding and controlling the structure and segregation behaviour of aurh nanocatalysts, Sci. Rep. 6 (2016) 1–8.